# Theoretical study of high-density phases of covalent semiconductors. II. Empirical treatment

Stewart J. Clark, Graeme J. Ackland, and Jason Crain
*Department of Physics, University of Edinburgh, Edinburgh, Scotland EH9 3JZ, United Kingdom*
(Received 14 May 1993)

We show that a simple pairwise model for covalent materials provides a good description of the high-density fourfold-coordinated metastable phases BC8 and ST12, in agreement with experimental results and *ab initio* calculations. We use this potential to study the high-pressure behavior and the free energy. We find that both phases are metastable at all temperatures. The relative energetic stability depends on the parametrization, but the ST12 phase has higher entropy. We therefore conclude that with correct pressure and temperature treatment it may be possible to synthesize ST12 as a high-density metastable phase in Si.

## I. INTRODUCTION

This paper continues our study of high-density metastable phases found in the tetravalent group-IV semiconductors, and comparison of our results with experimental[1] and *ab initio* calculations.[2] The phases are very long lived and can be produced by depressurization from the high-pressure metallic $\beta$-Sn phase.[3,4] Here we present a treatment based on empirical potentials which allows intuitive insights into the stability and pressure response of these materials, along with estimates of free energy to describe finite-temperature behavior. A detailed description of the structures and properties of these phases can be found in the introduction to the previous paper,[2] hereinafter referred to as Paper I. Projection diagrams of the atomic positions are also shown in Paper I.

In Paper I, we reported *ab initio* calculations based on density-functional theory in the local-density approximation. These calculations reproduced accurately the properties known experimentally, and furthermore gave some predictions for the exact behavior of the internal structure of BC8 and ST12 as a function of pressure.

Despite the success that density-functional (DF) total-energy calculations have had in describing the relative phase stability in crystals, there remain limitations which render the treatment of several important physical properties beyond that which can be achieved by these methods. This is particularly true in the case of free-energy calculations at finite temperature and relaxation of unit-cell dimensions under hydrostatic pressure. The explicit treatment of finite-temperature effects by first-principles methods is extremely difficult to incorporate in practice, although a rigorous extension of density-functional theory to finite temperature does exist. This is because of the long simulations required to obtain good thermodynamic averages, and the difficulties associated with changing the box volume with thermal expansion and fluctuations.

For structural relaxation, the plane-wave-pseudopotential total-energy method has been shown to alleviate substantially complications which arise in atomic-force calculations. These difficulties include basis-set corrections (Pulay forces), which must be considered when localized basis sets are used, and corrections which arise from non-self-consistency in the solution of the Kohn-Sham equation, which are particularly problematic in full-potential treatments. The advantages of the pseudopotential-plane-wave methods, however, do not apply in the case of unit-cell relaxation for noncubic systems, which remains a formidable task to implement by first principles. Schemes which have been proposed to accomplish this show extremely unfavorable scaling with system size.

These two complications associated with density-functional methods coupled with the urge to explore the $P$-$T$ diagram of dense metastable phases of Group-IV semiconductors have provided the motivation for the present work. In Paper I we reported *ab initio* pseudopotential DF calculations which accurately reproduced known structural properties and allowed for predictions as to the internal relaxation of the BC8 and ST12 structures of Group-IV elements under pressure. To make the thermodynamic problem more tractable, we have replaced the *ab initio* forces calculation with an empirical potential which reproduces the structural results.

With a view towards a full theoretical investigation of the $P$-$T$ diagram of these phases, including hydrostatic effects, we have first carried out the same analyses as in Paper I, using a previously published empirical model for covalent bonding.[5,6] This potential was parametrized to model quite different situations, such as the diamond structure and small clusters. It has, however, been shown to be successful in other regimes very different from that for which it was parametrized. It has previously been shown to provide an accurate description of defects, vibrational properties, rebonding effects in surface reconstructions, and in the formation of clusters. It has not been applied previously in the present context of dense phases of covalent semiconductors, so tests of its perfor-

0163-1829/94/49(8)/5341(12)/$06.00  

mance are essential. These results are compared to those of experiment, where available, or to those of the *ab initio* calculations reported in Paper I, and show remarkably good agreement.

The computer-intensive nature of density-functional calculations means that finite-temperature studies at many points in the phase diagram are currently impractical, especially in view of the pressure and temperature dependence of the $c/a$ ratio. To investigate the stability of the phases it is, however, necessary to evaluate free energies throughout the phase diagram. The empirical potential enables us to carry out this calculation for a model covalent material, whose properties are fitted as closely as possible to those of silicon.

This paper is divided into eight sections and is organized as follows. The empirical potential and its characteristics are described in the next section. This is followed by a description of the calculated structural properties of the BC8, ST12, and $\beta$-Sn phases and their relative response to applied pressure. A discussion of the $P$-$T$ diagram follows and is based upon separate discussions of the vibrational properties under pressure.

## II. DETAILS OF THE EMPIRICAL POTENTIAL

Much effort has been invested in deriving simple potential models for covalent materials such as silicon. The intuitive picture of a covalent bond suggests that pairwise interactions should dominate the structural properties, and yet no standard short-ranged pair potential stabilizes the diamond structure. Various methods have been introduced to circumvent this: several authors have introduced potentials with a strong angular dependence.[7,8,9] Pettifor[10] arrived at a similar solution from approximate tight-binding ideas. Models based on the notion of a bond charge,[11] or on a function of the local coordination[12] have also been tried. Most of these models were successful in the regime for which they were parametrized, but showed a lack of transferability. The final model of Tersoff perhaps comes closest to being transferable, but at the price of considerable functional complexity and 13 fitted parameters. A recent survey of six such potentials[13] concluded that each has strengths and limitations, none appearing clearly superior to the others, and none being fully transferrable.

For the present study we require a potential which gives a reasonable treatment of high-pressure phases and phonons, and can give an insight into the different behaviors of silicon and germanium. Recently, it has been shown that a very simple model, based on analytic pair potentials representing one bond per electron, gives good results in studies of phonons, high-pressure phases, surface reconstruction, defects, and cluster formation. An unusual aspect of this potential is its simplicity (three free parameters, two more to define length and energy scales) and its transferability.

In its parametrized form, this potential is written as follows:

$$E = \frac{1}{2}\sum_{i=1}^{N}\sum_{j=1}^{N} A(r_{ij}) - \frac{1}{2}\sum_{i=1}^{N}\sum_{k=1}^{4} B(r_{ik}) + \sum_{i=1}^{N}\sum_{n=1}^{3}\sum_{m=n+1}^{4} C(r_{k_m k_n}). \quad (1)$$

The function $A$ term represents the short-ranged repulsion due to core overlap. $B$ represents the covalent bonds themselves, the sum is interpreted as being over *electrons* but can be written as a sum over atom pairs (limited here to four neighbors per atom, though double bonds $k_m = k_n$ are allowed). $C$ represents the repulsion between adjacent bonds as the angle between them is reduced, due mainly to distortions in the orbitals to preserve orthogonality. Again, although the final term is interpreted as a sum over pairs of bonding electrons sharing a common atom, it can be written as a sum of pairwise interactions between pairs of neighbors of a given atom. Thus the rather complicated notation in which $k_m$ means the label of the $m$th neighbor of atom $i$.

There is no physical justification for the analytic form of the functions chosen to represent each term, so here we assume both they and their parameters to be the same as in the previous papers:

$$A(x) = Ae^{-\alpha x}, \quad (2)$$

$$B(x) = Bxe^{-\beta x}, \quad (3)$$

$$C(x) = C(\cos wx + \tfrac{1}{3})^2. \quad (4)$$

In general there is no unique way to select the four "bonded" neighbors (choosing the four nearest neighbors may not satisfy the requirement that if $i$ is bonded to $j$ then $j$ must be bonded to $i$). In the present case, however, we have fourfold-coordinated crystal structures so this difficulty does not arise.

The electronic-structure calculations also provide strong evidence that this model will not be suitable for modeling BC8 carbon, because that appears to be more like a molecular crystal. This is similar to the situation found in clusters,[6] where small silicon and germanium clusters form distorted structures maximizing their number of bonds (up to four). By contrast, rather than distort bond angles, small carbon clusters form rings and chains containing double bonds. This preference for double bonding rather than massively distorted bond angles is a qualitative difference between silicon and carbon. It is difficult for a single potential formalism to describe both behaviors.

Within the current model, the physical picture which explains the difference is that the bond bending arises primarily from orthogonalization within the atom core (which is why it runs over pairs of bonds to the same atom). In silicon the $3s3p^3$ valence electrons are kept away from the center by orthogonality to the $2s2p^3$ (this effect is even more pronounced in germanium), and consequently their overlap and attendant orthogonality contribution to bond-angle distortions are smaller. The con-

sequence of this is that in Si and Ge distorted tetrahedra are favored over double bonding.

This argument can be developed further to explain the differences between Ge and Si found in the previous paper. ST12 has bond lengths clustered more closely around the "ideal" (diamond) value than does BC8, but at the expense of a much wider spread of bond angles. Consequently, in germanium where smaller overlap allows for easier bond-angle distortion, the ST12 structure is favored. In silicon the bondbending is more costly, so the BC8 structure is found. Finally in carbon, with no core $p$ electrons, the orthogonalization cost of bond-angle distortion is too great for either ST12 or BC8, to form with true fourfold coordination.

A surprising aspect of this formalism is that it stabilizes the metallic sixfold-coordinated $\beta$-Sn structure at high enough pressures.[5] The absence of any metallic nature in the covalent formalism makes this stability surprising. The predicted $c/a$ ratio, however, is around 0.65, and highly pressure dependent. In silicon, it is 0.55 and almost independent of pressure. This discrepancy shows that the model is beginning to break down by failing to allow for the attraction of the two neighbors of each atom in the $c$ direction. It is fair to presume, therefore, that the cohesive energy of $\beta$-Sn may be underestimated, and we find evidence for that here in that the predicted diamond–$\beta$-Sn transformation pressure is greater than that for diamond-BC8.

Thus the model of Eq. (1) appears to meet our criteria for the current study. Throughout the paper we shall examine the discrepancies of its predictions with experiments, and what effect these discrepancies have on the accuracy of our final results. As we shall see, it reproduces the pressure behavior of the BC8, and ST12 phases well, and while it is less accurate for the absolute phonon frequencies than other potentials fitted for that purpose, these inaccuracies tend to cancel out when examining phase stability.

## III. STRUCTURAL DETAILS

Figure 1 shows the relative stability of diamond, ST12, BC8, and $\beta$-tin phases for the potential with parameters fitted to silicon. From these curves we can deduce the lattice parameter and cohesive energy for these phases (Table I). The graphs representing ST12 and $\beta$-Sn are under hydrostatic pressure, obtained by minimizing enthalpy with respect to all internal parameters and the $c/a$ ratio. Including these degrees of freedom makes a significant difference to the curve, softening the bulk modulus considerably.

Figure 2 shows a plot of the minimum cohesive energy of $\beta$-Sn parametrized by different fixed $c/a$ ratios. Notice here that the lowest point of this graph is identical to that of the diamond structure. This is because diamond can be regarded as $\beta$-Sn with a $c/a$ ratio of $\sqrt{2}$. The concave shape of the graph shows that under pressure silicon remains in the diamond structure rather than reducing its volume by becoming $\beta$-Sn with a smaller $c/a$ ratio, and shows also that the diamond–$\beta$-Sn transformation is first order. The implied transition pressure is 8.5 GPa, below which pressure the $\beta$-tin phase becomes unstable. The concave nature of the $\beta$-Sn curve also shows that, while a martensitic transformation proceeding by continuous reduction of $c/a$ is geometrically possible, it is kinetically unfavorable and could occur only with considerable hysteresis, requiring a pressure of at least 12.4 GPa (from the tangent at $c/a=\sqrt{2}$). Consequently, the model predicts that for a range of volumes no mechanically stable structure with $\beta$-tin symmetry exists at any hydrostatic pressure. For this reason, the $\beta$-tin curve in Fig. 1 does not continue to a turning point or to larger volumes. The actual transformation probably proceeds by a nucleation and growth process, perhaps involving partial dislocations.[14] In any case, its kinetics must be sufficiently complex to account for the nonobservation of the retransformation.

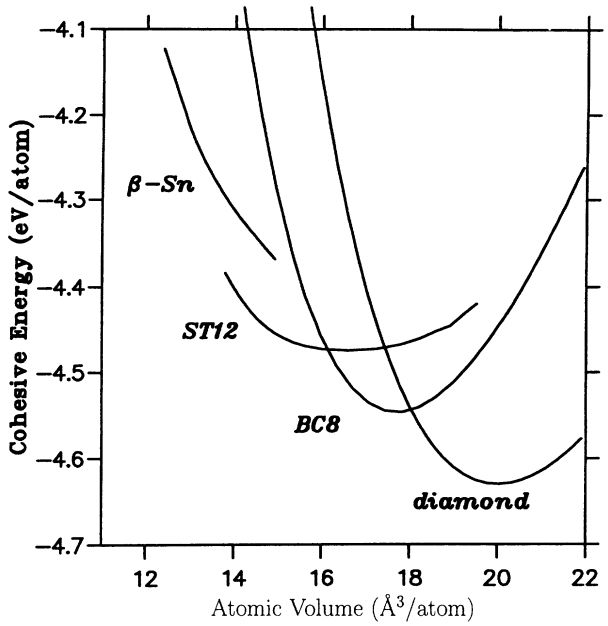


FIG. 1. Plot of energy against volume for various phases.

The potential can sometimes give rise to ambiguities in choosing the neighbors, especially if considerable relaxation is required after the choice has been made. BC8 has a single internal parameter to relax. It has four nearest neighbors and so there is no difficulty in determining the bonding arrangement $r_{ik}$. Although the fifth neighbor is relatively close, the charge-density plots in the previous paper confirm the assumption implicit in the form of the empirical potential that there is no bond to it.[2] If the fifth neighbor is included as one of the four bonds at the expense of the $B$ bond, it gives a higher energy structure.

TABLE I. Cohesive energies (eV/atom) and lattice parameters (Å) at zero pressure.

| Structure | Lattice constant(s) | Cohesive energy |
|---|---|---|
| Diamond | 5.429 | -4.631 |
| BC8 | 6.577 | -4.546 |
| ST12 | 5.761, 6.2546 | -4.475 |

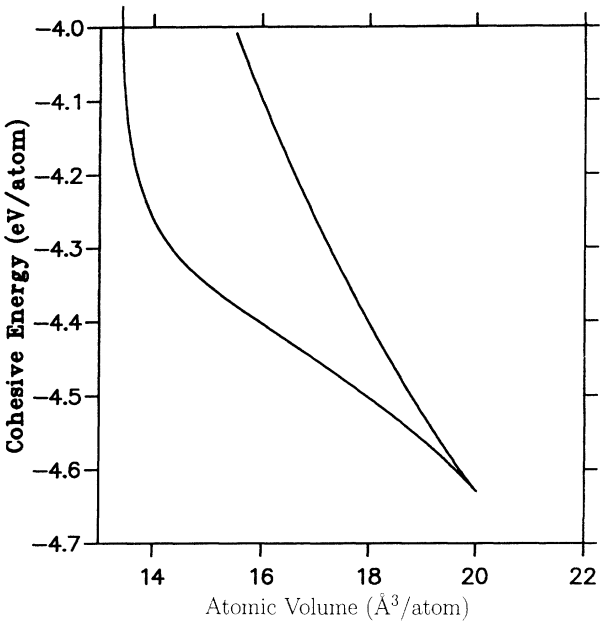


FIG. 2. Plot of the minimum energy for the $\beta$-Sn phase at a given $c/a$ ratio against the unit-cell volume at that energy and $c/a$ ratio.

Including it at the expense of the $A$ bond leads to massive increase in $x$, achieved by simulated annealing, back to a BC8 structure: the broken $A$ bond now becomes the new fifth neighbor.

ST12 has four internal parameters and two lattice parameters. The enthalpy is minimized with respect to all of these. Once again, it is a fourfold-coordinated phase and so there is no difficulty in selecting the correct bonding arrangement. As with BC8, the charge-density plots in Paper I give a clear indication that four covalent bonds is the correct description of the bonding.

## IV. EFFECT OF PRESSURE ON STRUCTURE

The diamond structure can respond to pressure only by contraction of its bonds, but pressure increase in BC8 and ST12 can be taken up by increased internal distortion, change in bond lengths, and change in $c/a$ ratio. In practice all these happen simultaneously.

Due to problems with changing basis sets, many *ab initio* calculations are unable to calculate forces and then relax the relative atomic positions. They are therefore restricted to rescaling all bond lengths. With a plane-wave basis set this problem is somewhat alleviated, and for a given unit cell the atomic position can be determined. This still does not fully allow for relaxation of $c/a$ ratio with pressure. By minimizing the enthalpy using a conjugate-gradients procedure with the Parrinello-Rahman Lagrangian,[15] it is possible to allow both internal and unit-cell parameters to relax simultaneously, as they would in a real material.

In Fig 3 we show the importance of including all degrees of freedom in the case of ST12. This can currently be done only with empirical potentials. The graph shows the change in length of the three distinct bonds with volume under full relaxation and under conditions of constant $c/a$. For reference, we show the variation of a typical bond length when no relaxation is allowed (it simply remains proportional to the cube root of the atomic volume).

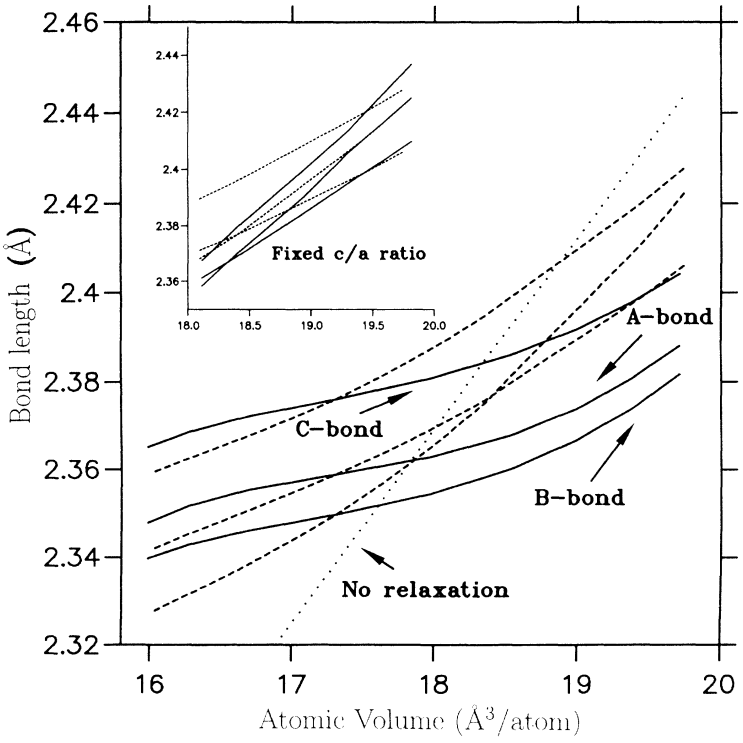


FIG. 3. Comparison of empirical bond lengths in ST12 with full relaxation (full lines), fixed $c/a$ ratio (dashed lines), and no relaxation (dotted line). Inset: Comparison between empirical and *ab initio* neighbor distances in ST12 as a function of pressure at fixed $c/a$ ratio.

It is clear that the change in $c/a$ with pressure is such as to reduce the necessary change in bond lengths. In both ST12 and BC8 the material is able to reduce its volume without commensurate reduction in bond lengths by adjusting its internal degrees of freedom. This has a very significant effect on the bulk modulus, which is lower in the denser phases than in diamond, in spite of a much greater number of bonds per unit volume.

Figure 4 shows the variation of the BC8 internal parameter $x$ with change in volume as determined by empirical methods. In Fig. 5 we show the variation in neighbor distances with decreasing volume comparing the empirical and *ab initio* results. We recall that the local-density approximation (LDA) invariably underestimates the lattice parameter of solids by about 2%, while the empirical model has its length scale set to reproduce the diamond structure exactly. Allowing for this, comparison with the *ab initio* simulation shows that the pressure evolution of the structure is well described by the model.

The crossover in BC8 bond lengths occurs with both empirical and *ab initio* methods, though at different pressures. The semiempirical model gives an intuitive explanation for this. The compression of the type-$A$ bond is restricted by repulsion arising from the orthonormality requirement with the type-$B$ bonds. Since the angle $\Theta_{AB}$ is smaller than $\Theta_{BB}$, the $AB$ overlap is greater than the $BB$ overlap, and so this term dominates the differential short-ranged repulsion. There are three times as many $AB$ angles to the $A$ bond as to the $B$ bond, so we expect its compression to be three times more difficult, and indeed that is what we observe in Fig. 5: the slope corresponding to $A$ is about a third that corresponding to $B$. An alternate way of rationalizing this is that relaxation of the internal parameter $x$ causes much larger changes in $A$ than in $B$ ($dA/dx = 2\sqrt{3}$; $dB/dx = (8x-1)/2B$), so while symmetry is retained internal relaxation can do little to affect $B$.

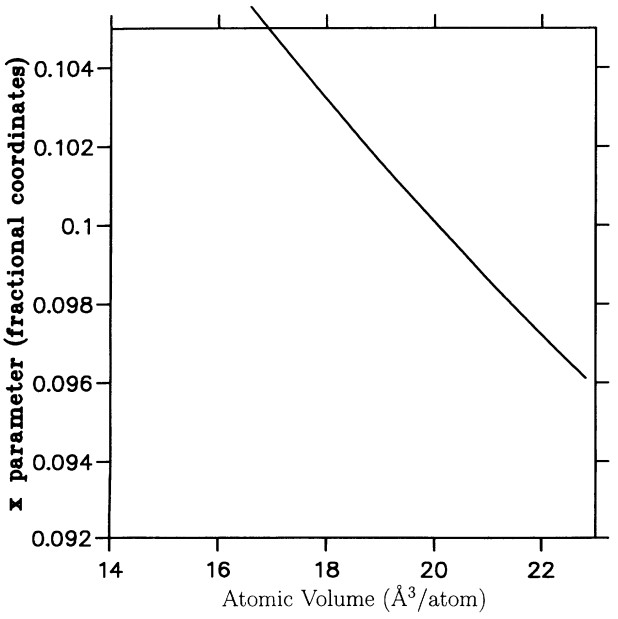


FIG. 4. Variation of the internal structural parameter $x$ of the BC8 structure with pressure.

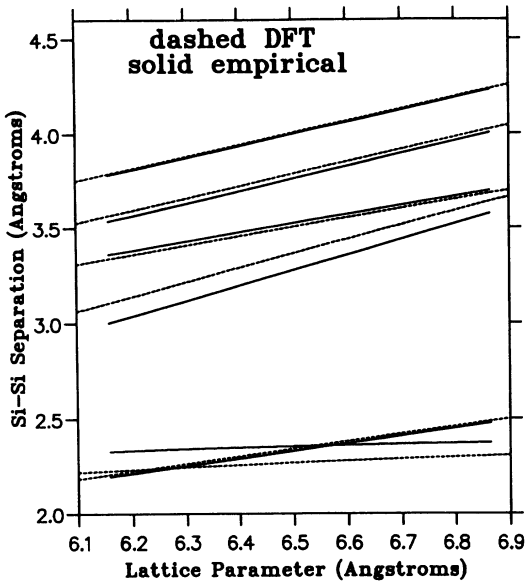


FIG. 5. Comparison between empirical and *ab initio* nearest-neighbor distances in BC8 as a function of lattice parameter.

ST12, has four internal degrees of freedom and, because of its tetragonal symmetry, two independent lattice parameters. Its space group is $P4_32_12$ ($D_8^4$) or its enantiomorph. In germanium ST12, the bond lengths are on average about 1% longer than in the diamond structure, which leads to a density about 10% greater. All the atoms are fourfold coordinated, and there are two distinct atomic environments $a$ and $b$. The eight type-$b$ atoms per unit cell form spiral chains with a unique helicity, bridged by the four type-$a$ atoms. We therefore expect ST12 to be optically active, although this has yet to be confirmed experimentally. A combination of sevenfold and fivefold rings means that the bond angles are much more diverse than in BC8, but also enables the bond lengths to be much closer to one another than in BC8.

We find that in addition to the internal parameters, the $c/a$ ratio varies as a function of pressure, so we use the Parrinello-Rahman Lagrangian[15] to investigate high-hydrostatic-pressure behavior. Simple scaling of the unit-cell parameters, adequate for diamond or BC8, would be incorrect in ST12 because of the pressure dependence of $c/a$.

With so many variables to consider, it is not obvious how best to represent the response to pressure. In the inset to Fig. 3 we compare the behavior of the three distinct "nearest-neighbor" bond lengths as a function of volume with $c/a$ held constant at the value which gives minimum energy at zero pressure. This ensures consistency in the degree of relaxation among the structures examined by the *ab initio* method. We compare the empirical result with results from Paper I because ST12 silicon has not been synthesized experimentally, but it

should be noted that while the empirical potential is fitted to the actual lattice parameter (of diamond silicon), LDA always gives too small a lattice parameter.

## V. PHONON SPECTRUM

The empirical potential has been used to calculate the phonon spectra for diamond, BC8, and ST12 phases at various pressures up to 10 GPa. Atomistic relaxations, as described in Sec. IV, have been performed under constant pressure, allowing the atoms and box size to relax into their equilibrium state. These atomic positions and cell parameters are used in conjunction with the potential to calculate the vibrational frequencies allowed in the crystals. To calculate thermodynamic properties, we require only the phonon-frequency density of states and not the entire dispersion curve, so we calculate the dynamical matrix of the complete cell used in the simulation treating it as a single cell.[16] This allows the actual Brillouin zone to be sampled at many $k$-points, giving a good representation of the density of states. We find that a cell consisting of $4 \times 4 \times 4$ unit cells (containing $N$=512, 768, and 1024 atoms for diamond, ST12, and BC8 respectively) results in a reasonable representation of the Brillouin zone. The dynamical matrices of size $3N \times 3N$ for the three relaxed structures, at various pressures from 0 to 10 GPa, are diagonalized to obtain the pressure-dependent phonon density of states. The entire phonon calculation was carried out on a CM200 Connection Machine. A full description of the procedure is documented in Ref. 17, along with a comparison between the potential used here and that of Stillinger and Weber.[7]

The phonon-frequency densities of states for diamond, BC8, and ST12 are shown in Fig. 6 for pressures of 0, 5, and 10 GPa. The general shape of the graph for diamond at the higher frequencies at ambient pressure is in good agreement with experiments on silicon.[18] There is a higher density of low phonon frequencies than that found[19] experimentally, although the values of these

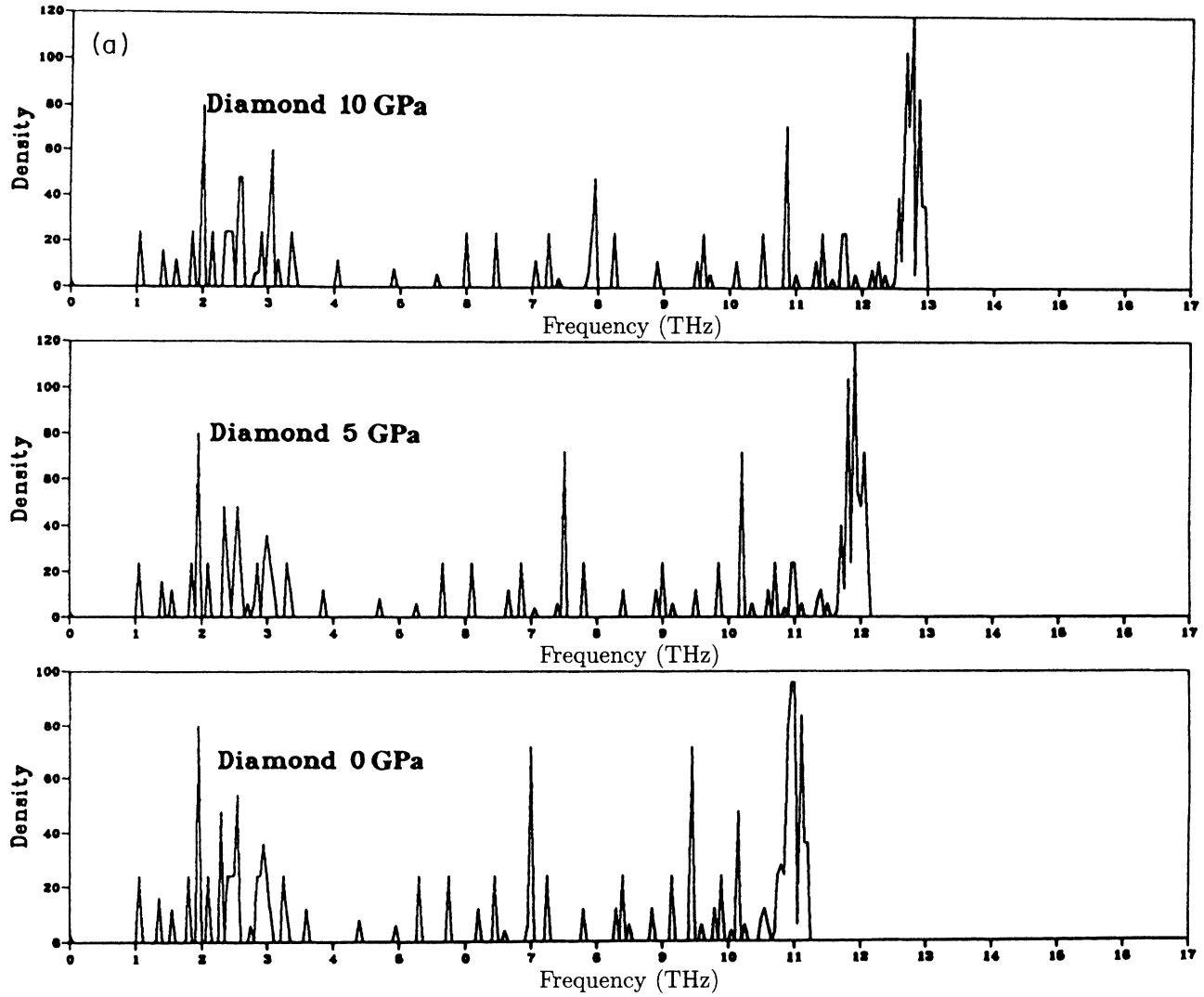


FIG. 6. Calculated phonon spectra for (a) diamond, (b) BC8, and (c) ST12 structures at pressures of 0, 5, and 10 GPa.

frequencies are in good agreement. The low-frequency modes are bond-bending modes and hence extremely sensitive to the $C$ parameter in the potential. We note that the same potential is here being used to give structural energies as well as phonon frequencies. There is no reason to expect that energies associated with bond distortion should be related to those arising from bond formation.

The largest numerical discrepancy with experimental results in silicon is the optic branch of the spectrum, where some of the frequencies are up to 30% too low. We have found that it is possible to rectify this by a reparametrization of the model, including these frequencies in the fitting procedure. This introduces some other discrepancies and we do not believe that the resultant model is any more similar to silicon than the original. It does, however, enable us to test how robust the formalism is, and how our results are affected by different parametrization. A reparametrization with the optic branch centered on 15.5THz,[18] with cohesive energy and diamond lattice parameter unaffected, resulted in a change of only 0.3% in the BC8 free energy and 0.1% in ST12 at 1000 K (and less at low temperatures). The effect on the BC8-ST12 free-energy difference at zero pressure ranged from 0.1% at 0 K up to 8% at 1000 K. The optic modes depend almost entirely on the bond-stretching forces, which are virtually the same in BC8 and ST12 due to their similar bond lengths. In comparing free energies, this systematic error tends to cancel out. This gives a physical explanation of the robustness of our results against typical errors introduced by the empirical model.

It is interesting to note that there is a range of forbidden frequencies in the higher range of the spectrum for the ST12 structure. As pressure increases, the gap increases from 0.5 THz at ambient pressure to almost 1.5 THz at 10 GPa.

We have picked out the frequencies of the zone-center phonons for comparison with Raman spectroscopy. The variation in frequency with pressure of zone-center phonons in BC8 [see Fig. 7(a)] is remarkably similar

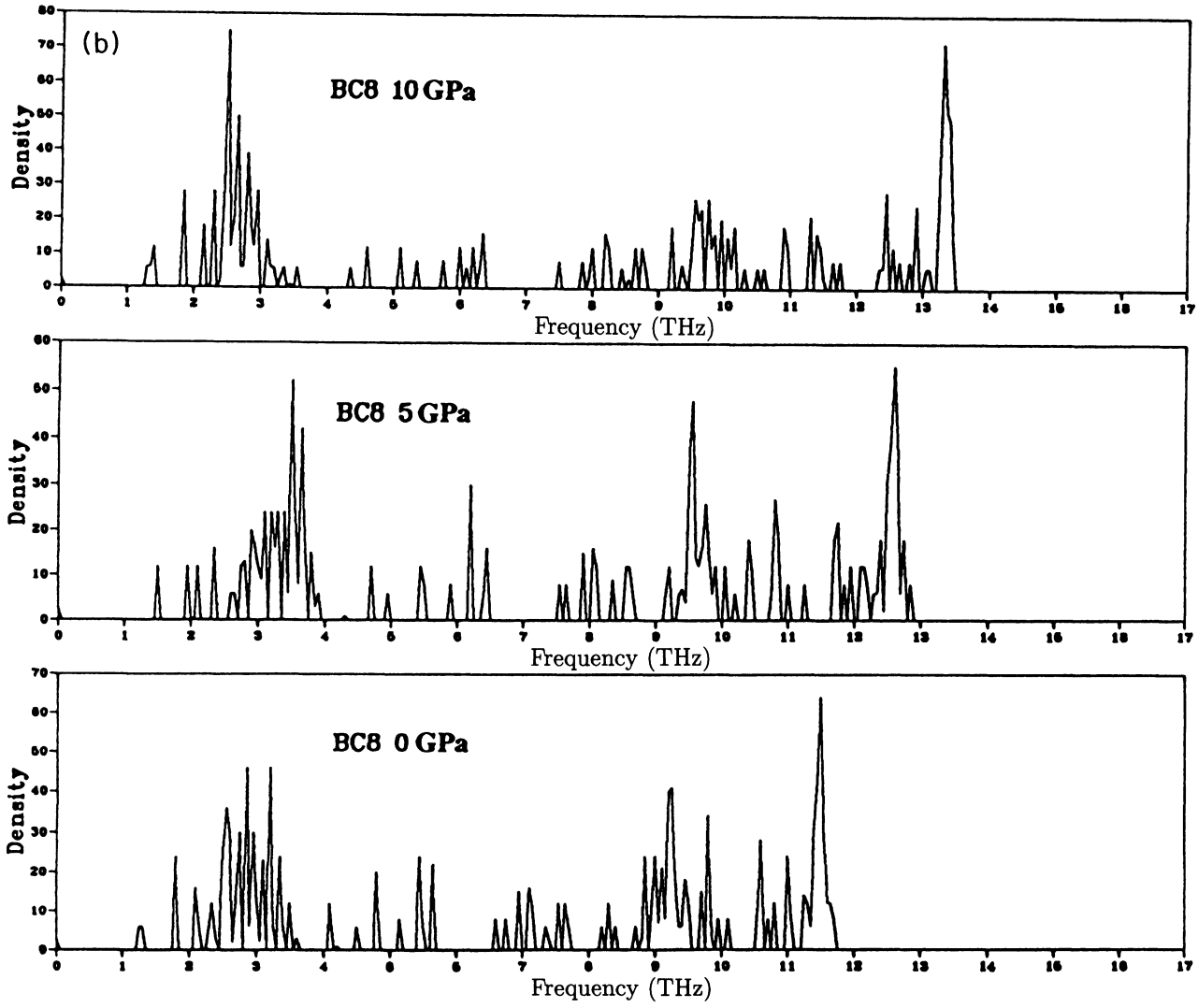


FIG. 6. (*Continued*).

to that measured experimentally in silicon.[20] We find that the low-frequency modes are almost unchanged with pressure, consistent with the TA phonons in most tetrahedral semiconductors. These may even be anomalous in that their frequency is slightly reduced with pressure. We associate the lack of anomalous modes in the simulation to the lack of explicit bond-length dependence in the term which describes the low-frequency modes. This implies that the effective force constants for these modes are unchanged or even slightly weakened by pressure, giving low or negative Grüneisen parameters. The Grüneisen parameters have been calculated for the zone-center modes shown in Fig. 7 and are shown in Table II. In Fig. 7(b) we plot the equivalent quantities for ST12. In this case there are no experimental data.

The predicted Gruneisen parameter for the diamond TA($X$) phonon is extremely small (0.15), only a tenth of that for bond-stretching modes, but non-negative. This mode is dominated by the bond-bending term, and the Grüneisen parameter is always positive for models with this type of bond-bending term, because the third derivative of $(\cos\theta + 1/3)^2$ is $\sin\theta(8\cos\theta + 2/3)$ which is negative for all angles occurring in BC8, ST12, and diamond.

Since the entropy calculation requires a sum of (logarithms of) frequencies, and not a product, the absolute error in this quantity, regardless of sign, is the important feature. This is small.

## VI. FREE ENERGIES

From the phonon calculation, we can calculate the temperature-dependent vibrational free energy and total vibrational energy associated with all three structures. Since we are able to calculate the phonon density of states we can simply obtain the partition function of the vibrations using Bose-Einstein statistics from which we can find the thermal properties of the structures in the harmonic approximation. Graphs of this temperature dependence are shown in Fig. 8 at ambient pressure. We notice that the vibrational free energy for ST12 is significantly lower than that for BC8, which contrasts with

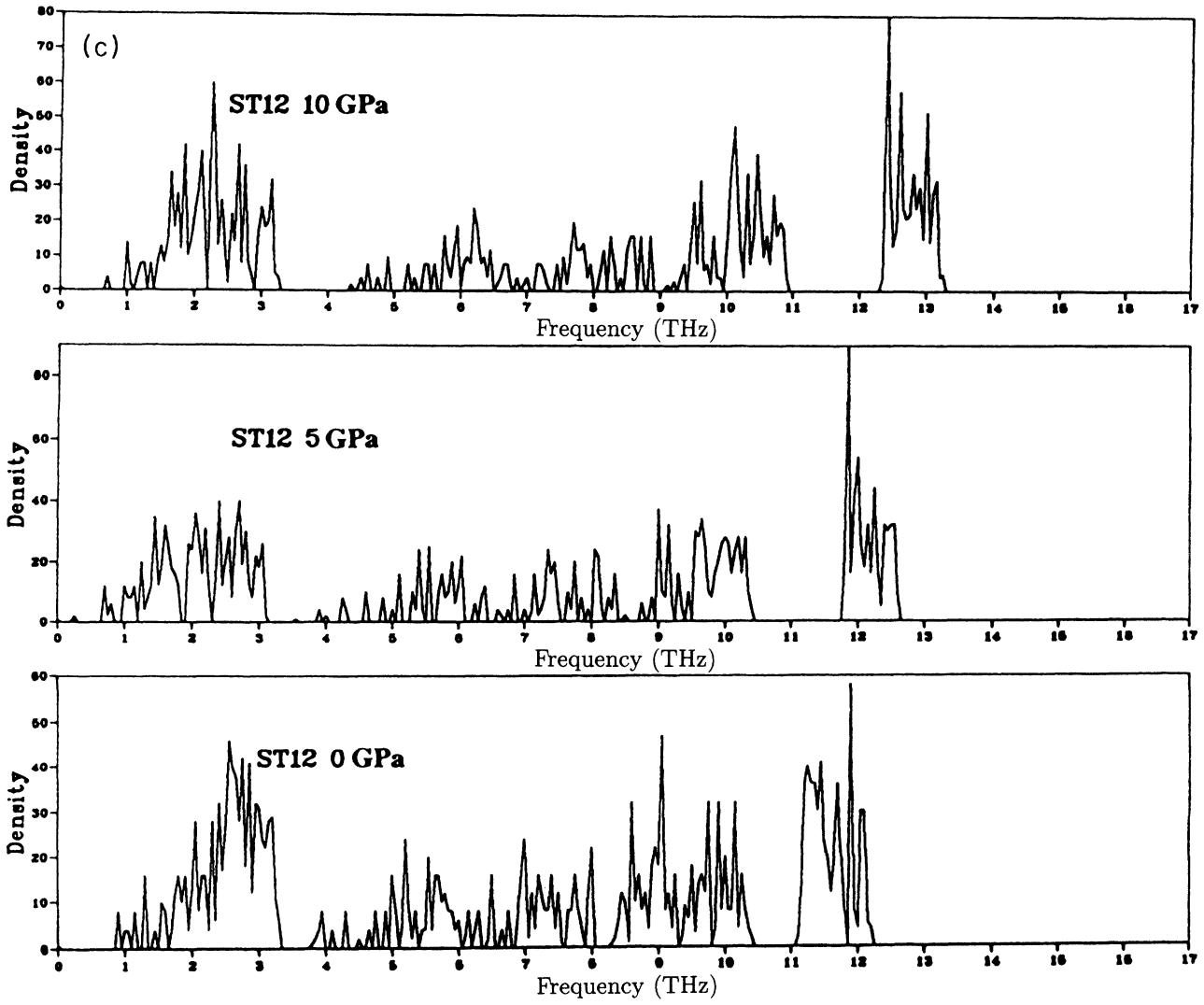


FIG. 6. (*Continued*).

the structural cohesive energy which is lower in BC8. Note that the difference in vibrational free energy for the BC8 and ST12 structures increases with temperature, and whenever this difference is larger than the difference in structural energy ST12 silicon will be favored.

We have applied our lattice-dynamics programs to these relaxed blocks, which has enabled us to span the entire pressure-temperature regime in calculations of free energy. We are therefore able to calculate the total free energy in the harmonic approximation:

$$G = U_{\text{struct}} + U_{\text{vib}} - TS + PV, \tag{5}$$

at all points in the pressure-temperature phase space for the ST12 and BC8 structures. The structural (cohesive) energy $U_{\text{struct}}$ and $PV$ can be obtained from either the *ab initio* or empirical molecular dynamics and the energy associated with the vibrations $U_{\text{vib}}$ and entropy $S$ are calculated from the statistics of the lattice vibrations. Note that the temperature dependence on volume is not included here since the harmonic approximation used in the lattice dynamics does not incorporate thermal expansion. The error in this assumption is relatively small since the volume of a tetrahedral semiconductor has a much greater response to pressure than to temperature. For a given temperature and pressure, the structure which has the highest total free energy $G$ will be favored.

Anharmonic contributions to the total free energy have been estimated from molecular-dynamics simulations at a range of temperatures using the empirical potential. These results were obtained from runs with an adapted version of the progam MOLDY[21,22] using 768 and 1024 atoms running for 25 000 time steps of 1 fs. Similar runs for diamond yield similar results. Both the absolute and differential contributions to the energy arising from anharmonic effects were found to be negligibly small, while calculating them is extremely demanding computationally. Consequently, we work throughout in the harmonic approximation for the vibrational properties.

It is possible to derive the specific heat capacity from these calculations, and in each case this was found to be $25 \pm 1.5$ J mol$^{-1}$, indistinguishable from the harmonic case. There is, of course, no electronic contribution to the heat capacity in this model. One useful anharmonic quantity which we do derive from the molecular dynam-

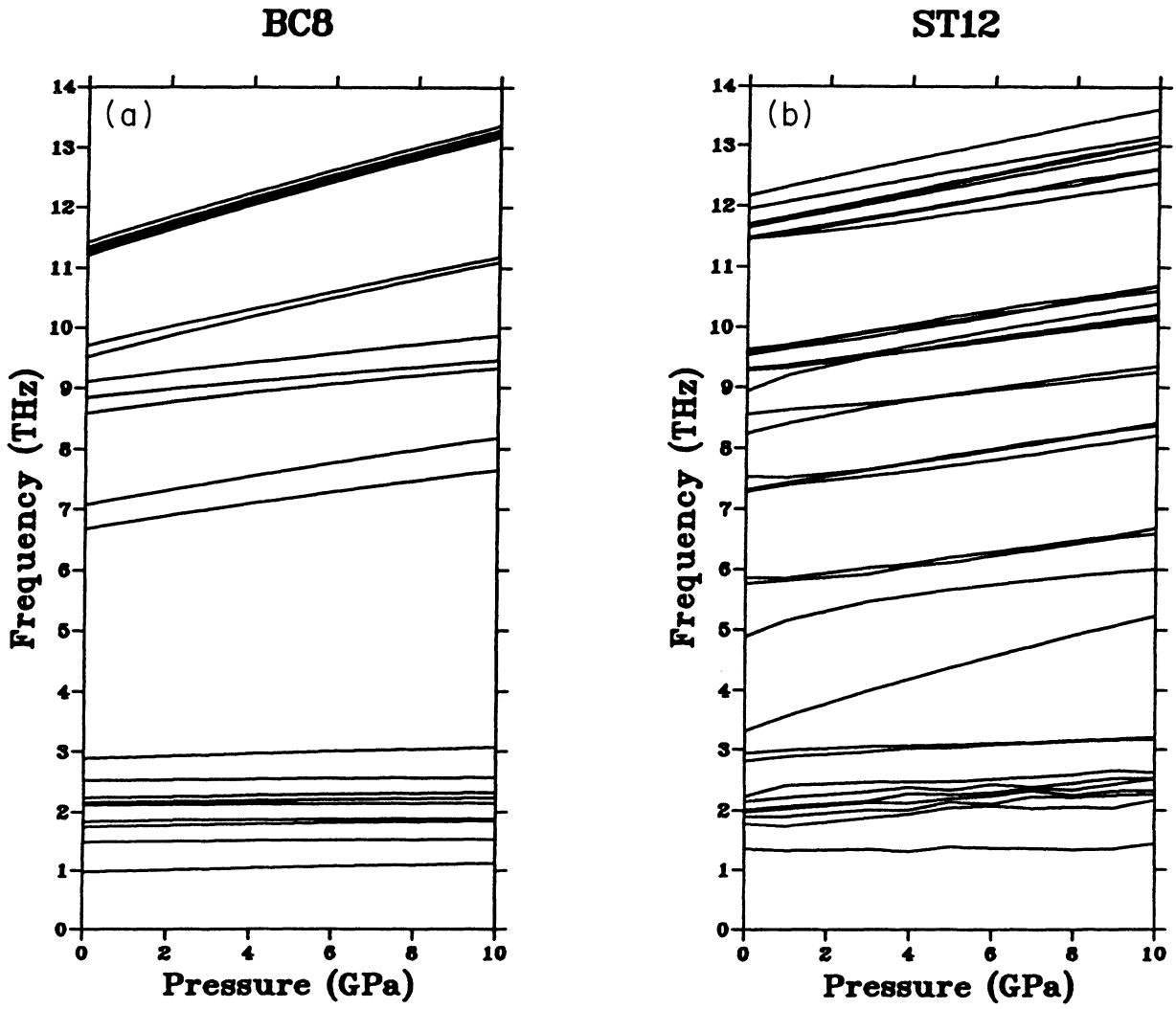


FIG. 7. Change in zone-center phonon frequencies with increase in pressure for (a) BC8 and (b) ST12 structures.

ics is the thermal expansivity of the two structures. The behavior of the third derivative is not included in the fit, so we would not expect the expansivity to be very well reproduced by the potential. However, we expect the trend observed from the diamond phase through BC8 to ST12 to be correct. We found values of $12 \pm 4 \times 10^{-6}$ K$^{-1}$ and $11 \pm 2 \times 10^{-6}$ K$^{-1}$ for BC8 and ST12 respectively. These are somewhat smaller than the value for diamond of $14.5 \times 10^{-6}$ K$^{-1}$ (about 20% higher than experiment). We are unaware of any experimental measurement of expansivity in the metastable phases.

The empirical model predicts the difference in structural energy $U_{\text{struct}}$, to be larger than in the *ab initio* calculations for silicon. This will affect the position of the stability field boundary in the phase diagram. For internal consistency we have used the empirical potential throughout to calculate a full pressure-volume phase diagram for ST12 and BC8 silicon, which is shown in Fig. 9.

The main contribution to the vibrational free energy comes from the low vibrational frequencies. These are mostly the bond-bending modes, which are determined by the $C$ parameter in the final term of the potential. Reduction in the $C$ parameter softens these modes and therefore increases the vibrational free energy. Hence for lower $C$ the minimum temperature at which the ST12 structure is more favorable is lowered. The first two terms in the potential essentially determine the depth, curvature, and position of the minimum of the structural energy of a tetrahedrally bonded crystal, and therefore a simple rescaling could be used to give a germaniumlike potential which in effect would weaken the bond stretching and lower the corresponding phonon frequencies. As noted above, this would retain the general shape of the phase diagram, but lower the temperature required to favor the ST12 structure. However, the bond-bending term in germanium will be even more significantly reduced, an effect which can be traced back to the smaller overlap of $4s4p^3$ orbitals on distortion. This also lowers the temperature and the pressure at which the ST12 structure will become stable over BC8. It makes ST12 germanium the metastable depressurized structure at room temperature. It therefore seems likely to be the case that BC8 germanium will be favored only at low temperatures and low pressures, perhaps forming on rapid depressurization.

TABLE II. Grüneisen parameters for the modes shown in Fig. 7 for silicon in the BC8 and ST12 structures.

| BC8 | ST12 |
|---|---|
| 0.51 | 0.59 |
| 0.47 | 1.63 |
| 0.88 | 1.66 |
| 0.35 | 1.36 |
| 0.25 | 1.82 |
| 0.58 | 1.37 |
| 0.57 | 1.20 |
| 0.29 | 1.01 |
| 0.99 | 0.76 |
| 2.15 | 3.80 |
| 2.31 | 1.51 |
| 1.31 | 1.34 |
| 1.06 | 1.33 |
| 1.25 | 1.09 |
| 2.44 | 1.22 |
| 2.23 | 1.14 |
| 2.57 | 0.92 |
| 2.56 | 0.56 |
| 2.54 | 0.95 |
| 2.52 | 0.83 |
| 2.49 | 0.89 |
| | 1.04 |
| | 0.97 |
| | 0.97 |
| | 0.95 |
| | 0.73 |
| | 0.86 |
| | 0.86 |
| | 0.96 |
| | 1.01 |
| | 1.01 |
| | 0.87 |
| | 1.01 |

## VII. DISCUSSION

The agreement between experimental, *ab initio*, and empirical results for the structural properties of high-density phases of Si and Ge gave us confidence to proceed with empirical calculation of a scale beyond what can be achieved by *ab initio* techniques. As a result of our calculations we find that, for a model whose parameters are fitted to describe silicon, the BC8 structure becomes unstable with respect to ST12 at high temperature and pressure.

We note that both phases are metastable with respect to diamond. Since they have very different topologies from one another, it seems unlikely that a simple kinetic path between BC8 and ST12 will exist. Consequently it will not be possible to transform BC8 into ST12 directly by heating–a more likely result is that the BC8 will simply transform into the true stable state, diamond, or to yet another metastable state, Lonsdaleite.[3] However, in view of the kinetic difficulty in transforming from $\beta$-Sn to diamond, it may be possible to depressurize silicon from the $\beta$-Sn phase at high temperature to a pressure above 6 GPa to form ST12 silicon.

Although the empirical model has not been explicitly parametrized for germanium, it is possible to make some general comments. The parameter $C$ governs the shear moduli and the vibrational frequency of the low-frequency phonons. In germanium the shear moduli are considerably smaller than in silicon, so a smaller value of $C$ would be appropriate. This would lead in turn to a downscaling of the phonon frequencies, and therefore of the entropies and entropy difference. In germanium, therefore, we would expect that the transition temperature should be much lower than in silicon–perhaps below room temperature. Thus it might be possible to produce BC8 germanium by depressurization below room temperature.

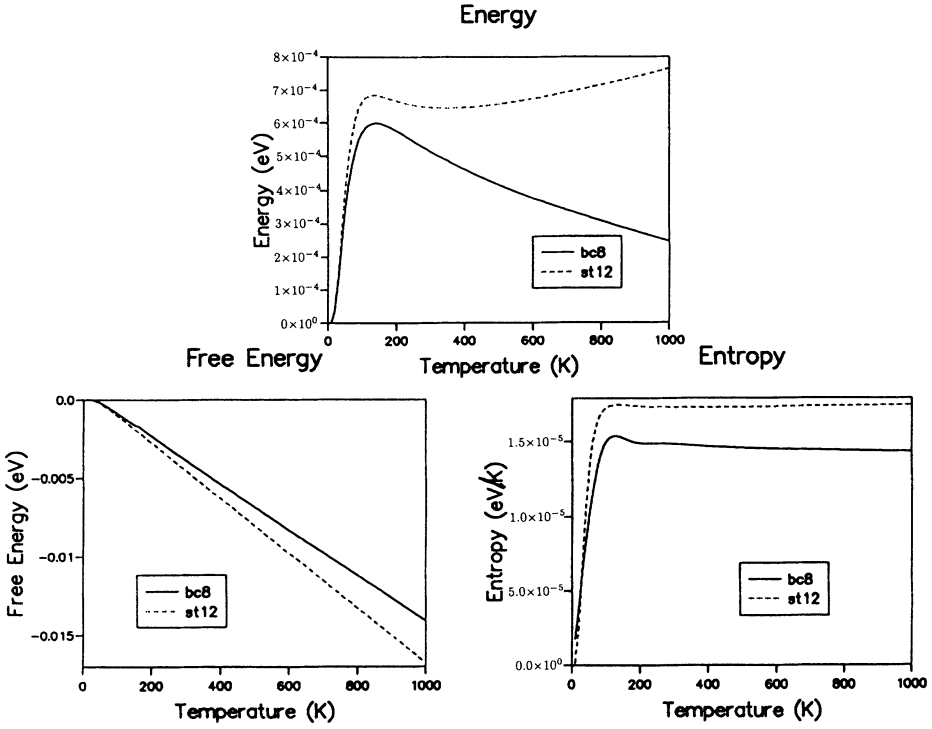


FIG. 8. Vibrational free energies as a function of temperature evaluated in the harmonic approximation for ST12 and BC8 structures at zero pressure. The vibrational free energies, total energies, and entropies for diamond are taken to be the zero of the calculations.

## VIII. CONCLUSIONS

The structural properties of BC8 and ST12 silicon and germanium are well described by a model designed for covalently bonded materials. This suggests that, although the electrical properties of BC8 may be dominated by a small Fermi surface, the primary contribution to bonding comes from covalent bonds. The same model can then reliably be used to determine phonon spectra, based on the covalent concepts of bond bending and bond stretching.

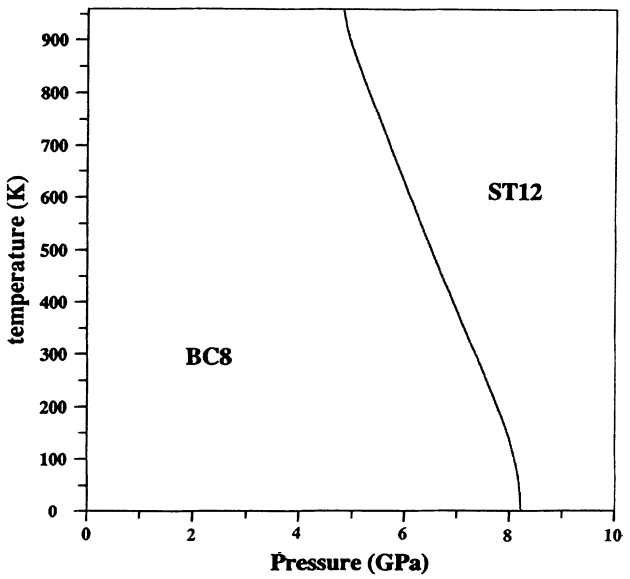


FIG. 9. Relative stability fields of ST12 and BC8 structures for silicon calculated from the vibrational free energies for ST12 and BC8 as a function of temperature and the structures found under pressure from the molecular-dynamics simulations.

Although both structures are based on covalent bonding, the bulk moduli are lower in the denser phases than in diamond. This is because they are able to contract both by bond shortening and bond bending, whereas diamond can contract only by bond shortening. As noted previously,[6] both silicon and germanium can be described with this model, the main difference being that the ratio of bond bending to bond stretching forces is lower in germanium.

The ST12 structure has a wider spread of bond angles but more closely matched bond lengths. Its many degrees of freedom allow it to take up external pressure with internal relaxations, giving it a large compressibility. These internal modes also give rise to many low-frequency phonon modes, making ST12 a high-entropy structure and therefore favored at high temperature and in germanium, where the large bond-bending distortions are least unfavorable.

Both ST12 and BC8 germanium have been reported, but the conditions in which they were made are not clearly documented and seem to lack reproducibility. ST12 silicon has not yet been found. Our calculations suggest that by conducting high-pressure experiments at different temperatures, the preferred phase can be altered. In particular, it may be possible to synthesize ST12 silicon by depressurization from $\beta$-tin at high temperature.

## ACKNOWLEDGMENTS

We would especially like to thank P. D. Hatton for many useful discussions regarding the experimentally

known structures in silicon and germanium. We would also like to thank Professor R. J. Nelmes for making his germanium results available to us prior to publication. G.J.A. would like to thank BP and the Royal Society of Edinburgh for support. S.J.C. and J.C. thank the SERC for support. We have also received considerable assistance from the Edinburgh Parallel Computing Centre on whose Connection Machine the phonon calculations were carried out.

[1] J.S. Kasper and S.M. Richards, Acta. Cryst. **17**, 752 (1964).
[2] J. Crain, S.J. Clark, G.J. Ackland, M.C. Payne, V. Milman, P.D. Hatton, and B.J. Reid, preceding paper, Phys. Rev. B. **49**, 5329 (1994).
[3] J.M. Besson, E.H. Mokhtari, J. Gonzalez, and G. Weill, Phys. Rev. Lett. 59, 473 (1987).
[4] R.J. Nelmes, M.I. McMahon, N.G. Wright, D.R. Allan, and J.S. Loveday, Phys. Rev. B **48**, 9883 (1993).
[5] G.J. Ackland, Phys. Rev. B **40,** 10351 (1989).
[6] G.J. Ackland, Phys. Rev. B **44,** 3900 (1991).
[7] F.A. Stillinger and T.A. Weber, Phys. Rev. B **31**, 5262 (1985).
[8] R. Biswas and D.R. Hamman, Phys. Rev. Lett. **55,** 2001 (1985); Phys. Rev. B **36**, 6434 (1987).
[9] M.I. Baskes, Phys. Rev. Lett. **59**, 2666 (1987).
[10] D.G. Pettifor, Phys. Rev. Lett. **63,** 22 (1989).
[11] D.W. Brenner and B.J. Garrison, Phys. Rev. B **34**, 1304 (1985).
[12] J. Tersoff, Phys. Rev. Lett. **56**, 632 (1986); Phys. Rev. B **37**, 6991 (1988); Phys. Rev. B **38**, 9902 (1988).
[13] H. Balamane, T. Halicioglu, and W. A. Tiller, Phys. Rev. B **46**, 2250 (1992).
[14] J. Crain, G.J. Ackland, P.D. Hatton, and R.O. Piltz, Phys. Rev. Lett. **70**, 814 (1993).
[15] M. Parrinello and A. Rahman, Phys. Rev. Lett. **45,** 1196 (1980).
[16] M. Born and K. Huang, *Dynamical Theory of Crystal Lattices* (Oxford University Press, Oxford, 1956).
[17] S.J. Clark and G.J. Ackland, Phys. Rev. B **48,** 10899 (1993).
[18] R. Tubino, L. Piseri and G. Zebri, J. Chem. Phys. **56**, 1022 (1972).
[19] W. Weber, Phys. Rev. B **15**, 4789 (1977).
[20] M. Hanfland and K. Syassen, High Pressure Res. **3**, 242 (1990).
[21] G.J. Ackland, D. Phil. thesis, Oxford University, 1987.
[22] M.W. Finnis (unpublished).